Central Lancashire Online Knowledge (CLoK)

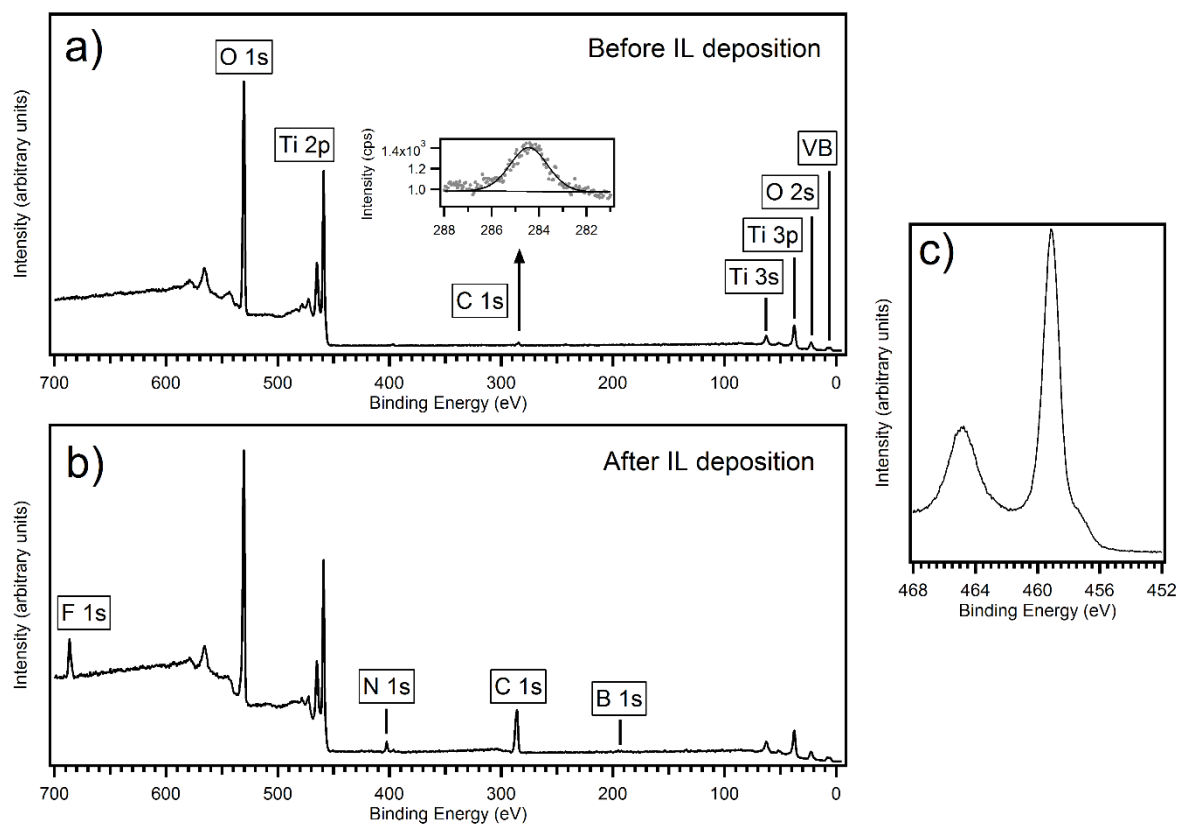| Title	Water-Induced Reordering in Ultrathin Ionic Liquid Films
Type	Article
URL	https://clok.uclan.ac.uk/23626/
DOI	https://doi.org/10.1088/1361-648X/aad24f
Date	2018
Citation	Henderson, Zoe, Walton, Alex, Thomas, Andrew G and Syres, Karen orcid iconORCID: 0000-0001-7439-475X (2018) Water-Induced Reordering in Ultrathin Ionic Liquid Films. Journal of Physics: Condensed Matter, 30 (33). ISSN 0953-8984
Creators	Henderson, Zoe, Walton, Alex, Thomas, Andrew G and Syres, Karen

It is advisable to refer to the publisher's version if you intend to cite from the work.
https://doi.org/10.1088/1361-648X/aad24f

For information about Research at UCLan please go to http://www.uclan.ac.uk/research/

Water-Induced Reordering in Ultrathin Ionic Liquid Films

Supporting Information

Survey spectra and Ti 2p spectrum under UHV conditions

Figure S1. *Survey spectra of the sample in UHV before IL deposition* **(a)** *and after IL deposition* **(b)**. *The Ti 2p region of the TiO₂ surface in UHV before IL deposition is shown in* **(c)**.

Calculation of inelastic mean free path of [C$_4$C$_1$Im][BF$_4$]

The inelastic mean free path (IMFP) of photoelectrons from [C$_4$C$_1$Im][BF$_4$] was calculated using the formula for organic materials by M. P. Seah [1]:

$$\lambda_{IL} = \frac{(4 + 0.44 Z_{IL}^{0.5} + 0.104 E^{0.872}) a_{IL}^{1.7}}{Z_{IL}^{0.3}}$$

Where Z_{IL} is the average number of protons from one ionic liquid (IL) pair, E is the maximum kinetic energy of photoelectrons from the TiO$_2$ substrate, and a_{IL} is the cube root of the IL's atomic volume. The IMFP, λ_{IL} = (2.6±0.2) nm for [C$_4$C$_1$Im][BF$_4$].

The average number of protons from one ionic liquid (IL) pair, Z_{IL}, was calculated using:

$$Z_{IL} = \frac{c Z_C + n Z_N + b Z_B + f Z_F}{(c + n + b + f)}$$

Where c, n, b, and f are the number of C, N, B and F atoms in one IL pair; and $Z_{C,N,B,F}$ is number of protons in C, N, B and F. Z_{IL}=3.9 for [C$_4$C$_1$Im][BF$_4$].

The maximum kinetic energy of photoelectrons from the TiO$_2$ substrate in eV, E, was calculated using the mean of the maximum kinetic energy of photoelectrons emitted from the O in the TiO$_2$. Each maximum kinetic energy was calculated using the energy of the X-ray photons from an Al Kα source (1486.6 eV) and the binding energy of the O 1s region (530.2 eV), which were acquired from the normalised in situ X-ray photoelectron spectroscopy data. For this study, E was found to be 956.4 eV.

The IL atomic volume in nm^3, a_{IL}^3, was calculated using:

$$a_{IL}^3 = \frac{10^{21} M_{IL}}{\rho_{IL} N_A (c + n + b + f + h)}$$

Where M_{IL} is the molecular mass of one IL pair (for [C$_4$C$_1$Im][BF$_4$], M_{IL}=226), ρ_{IL} is the density in gcm^{-3} of the IL (ρ_{IL}=1.2gcm^{-3} for [C$_1$C$_4$Im][BF$_4$] [2]), N_A is Avogadro's constant, and h is the number of H atoms in one IL pair. For [C$_4$C$_1$Im][BF$_4$], a_{IL}^3=0.0104 nm^3.

Calculation of film thickness of [C$_4$C$_1$Im][BF$_4$]

The film thickness of the ultrathin film of [C$_4$C$_1$Im][BF$_4$] in nm, d_{IL}, was calculating using the following (derived from the Beer-Lambert law [3, 4]):

$$d_{IL} = -\lambda_{IL} \ln \left(\frac{I}{I_0} \right)$$

Where λ_{IL} is the inelastic mean free path of photoelectrons from [C$_4$C$_1$Im][BF$_4$] in nm (for calculation of this, see previous section), I is the intensity of the O 1s signal from the TiO$_2$ substrate after IL deposition, I_0 is the intensity of the O 1s signal from the TiO$_2$ substrate prior to IL deposition. For this ultrathin deposition of [C$_4$C$_1$Im][BF$_4$], d_{IL}= (10±1) Å.

The number of layers was calculated by dividing d_{IL} by the 'thickness' of one [C$_4$C$_1$Im][BF$_4$] pair. The thickness of one [C$_4$C$_1$Im][BF$_4$] pair was assumed to be ~4 Å, which is in good agreement with Mezger and coworkers [5].

1-butyl-3-methylimidazolium tetrafluoroborate on anatase TiO$_2$ (101) and O 1s assignments

Measurements were taken of [C$_4$C$_1$Im][BF$_4$] on anatase TiO$_2$ (101), prior to the measurements examined in the main text. This data was not included in the main text due to beam damage. The IL, [C$_4$C$_1$Im][BF$_4$] was deposited onto an anatase TiO$_2$ (101) single crystal. Instead of one regime of exposure to water, this system was exposed to two different relative humidities with the same water vapour pressure. The first regime was exposure to 6 mbar of water at 20°C, corresponding to a relative humidity (RH) of ~20%. The second regime was exposure to 6 mbar of water vapour at 7°C, corresponding to RH ~60%. Between these measurements, the system was left to pump to ultra-high vacuum (UHV) overnight.
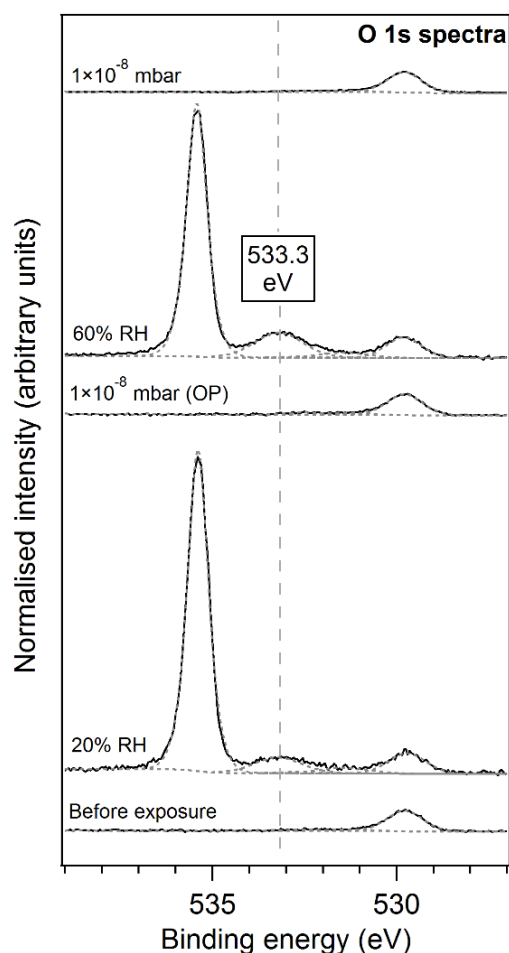

Figure S2. *O 1s spectra of [C$_4$C$_1$Im][BF$_4$] on anatase TiO$_2$ (101) before exposure to water, during exposure to water at 20% RH, under UHV after overnight pumping (OP), during exposure to water at 60% RH, and again under UHV conditions after the second exposure.*

Fig S2 shows the O 1s spectrum recorded during both of these regimes, alongside measurements taken before any exposure to water, after pumping to UHV, and after pumping to UHV again after the second exposure regime. The peak assigned to molecular adsorbed water is much more visible here than in the data presented in the main text. This is due to the intensity of the gas-phase water peak being much less than that of gas-phase peak in the main study. This peak also appears at 533.3 eV- the same binding energy of that assigned to adsorbed water in the main study.

N 1s spectra

Figure S3a shows the N 1s spectrum before exposure to water, and can be fitted with three peaks: the largest peak, situated at 402.3 eV is assigned to N in the imidazolium ring of the cations [6]. The peaks at 400.9 eV and 399.6 eV have been assigned as beam damage species, the binding energies of which are consistent with peaks associated with beam damage species observed by Wagstaffe et al [6].
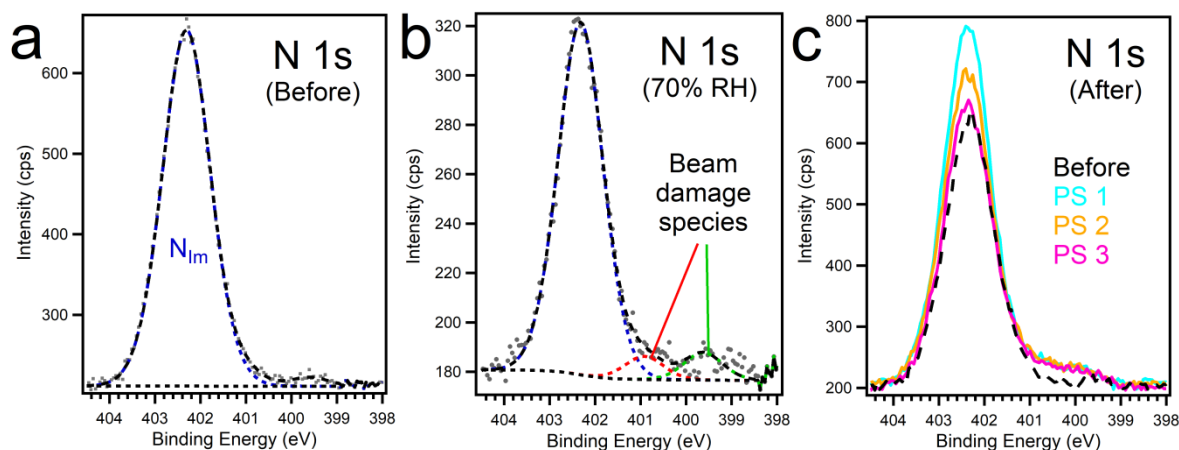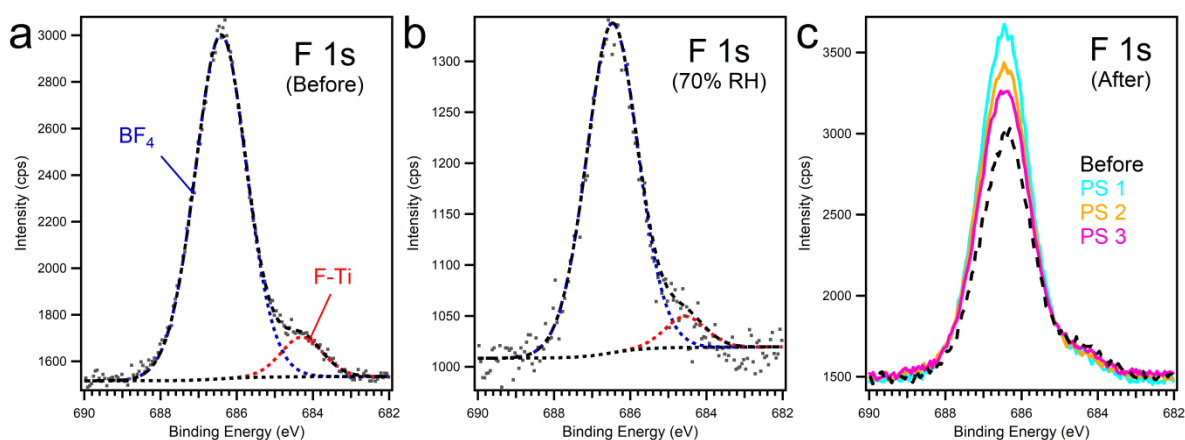

Figure S3. (a) *N 1s spectrum before water exposure,* **(b)** *N 1s spectrum at 70% RH, and* **(c)** *N 1s spectra throughout PS 1 to PS 3.*

Fig S3b shows the N 1s spectrum at 70% RH. No new peaks appear upon exposure, and the peaks at 400.9 eV and 399.6 eV increase in relative intensity (with a combined percentage of the N 1s region due to beam damage of 11%, compared to a combined percentage of 4% prior to water exposure). A theoretical study conducted by Mele et al [7] into the interactions between imidazolium-based ILs and water revealed that water interacts with the cation at the imidazolium carbons as they are capable of hydrogen bonding. It was also proposed that the presence of water separated the cation and anion species, replacing the cation/anion interaction. It is not clear whether a similar interaction has occurred here from either the N 1s or C 1s data. The peaks in the N 1s spectrum do not show any indication of returning to their original intensity values during PS 1 to PS 3. This confirms that these peaks are a result of damage to the sample from prolonged X-ray exposure. This behaviour has been observed in XP spectra of other imidazolium based ILs [6, 8]. Conversely, there is no evidence of beam damage in the C 1s or F 1s spectra. For further discussion on beam damage, see later in the SI.

F 1s spectra

Fig S4a shows the F 1s spectrum before exposure to water, and can be fitted with two peaks: the peak at 686.4eV arises from the F in the tetrafluoroborate ion [6, 9]. As mentioned in the main text, the smaller peak at 684.3eV is thought to arise from F-Ti bonding at the IL/TiO$_2$ interface [6]. In the work by Wagstaffe et al with the same IL on anatase TiO$_2$ (101) [6], the peak associated with F-Ti bonding makes up approximately 56% of the F 1s signal. In our study, this peak only makes up approximately 9% of the F 1s signal, which emphasised that the thickness of our IL film is greater than the (approximately) monolayer IL film studied by Wagstaffe.

Upon water exposure, the relative intensity of the peak associated with the anion increases (from 91% to 93%), while the peak associated with the F-Ti bonding decreases (from 9% to 7%). The decreased relative intensity could be the result of an attenuation effect, whereby the adsorbed water has increased the depth of the sample, resulting in an attenuation of the F-Ti signal from the buried IL/TiO$_2$ interface.

Figure S4. (a) *F 1s spectrum before exposure to water,* **(b)** *F 1s spectrum at 70% RH, and* **(c)** *F 1s spectra from PS 1 to PS 3.*

As water is evacuated from the system, the molecular adsorbed water eventually desorbs from the surface, and the peak associated with the BF$_4^-$ anion begins to decrease.

Cammarata et al [10] showed, using attenuated total reflectance infrared spectroscopy, that water interacts with the [BF$_4$]$^-$ anion via hyrdrogen bonding, both in imidazolium- and non-imidazolium-based ILs. This finding was also corroborated by Baldelli's group [11] using the

more surface sensitive technique of sum-frequency generation spectroscopy, who examined the interactions and surface orientation of $[C_4C_1Im][BF_4]$ and water. Ridings et al [12] used neutral impact collision ion scattering spectroscopy to show that small amounts of water in an imidazolium-based IL (1-hexyl-3-methylimidazolium chloride, $[C_6C_1Im][Cl]$,) can influence the composition of the IL surface. They found that at higher water concentrations the anion showed an increased presence at the IL surface, with the alkyl chains of the cation moving towards the bulk. Hence, as the water content is increased the charge at the surface becomes more negative. They attribute this behaviour to the influence of water on the hydrogen bonding network in the IL, specifically hydrogen bonding between the anions and water. While we do not see any evidence of bonding between the water and the BF_4^- ions in the F 1s spectra, we do observe a relative intensity change that suggests a rearrangement of the anion preferentially towards the IL/water interface. This somewhat corroborates the idea that water adsorbed on the IL influences the composition of the surface ions, bringing the anion and imidazolium ring toward the IL/water interface. However, these data are not the result of observation of the IL/water interface with a water-miscible IL. The data presented here, while appear to agree well with the findings of the study of $[C_6C_1Im][Cl]$ and water, are from an ultrathin sample of IL; not surface-sensitive measurements of bulk IL combined with water.

Atomic percentage concentration calculations

The concentrations of C, O and Ti were calculated for the TiO$_2$ surface prior to IL deposition using the total areas of each region and the associated relative sensitivity factor (RSF) for that element. The uncertainties have been calculated using the standard deviation of the region area in CasaXPS.

Table S1. *Composition (in atomic percentage) of C, O and Ti on the rutile TiO$_2$ (110) single crystal substrate prior to ionic liquid deposition.*

Region	RSF	Composition (%)
C 1s	1.00	2.3±0.6
O 1s	2.93	70.4±0.6
Ti 2p	7.81	27.3±0.3

The concentrations of C, N and F were also calculated for the ultrathin film before exposure to water and at PS 1. These are shown below with their associated uncertainties in Table S2. The peak areas of the C 1s, N 1s and F 1s regions at PS 1 were used as the rearrangement of ions was most prevalent at PS 1. Also displayed are the concentrations for C, N and F for bulk IL. The values adapted from Ref [13] were originally calculated using high-resolution XPS spectra of bulk [C$_4$C$_1$Im][BF$_4$].

Table S2. *Composition (in atomic percentage) of C, N and F in the sample before exposure to water and at PS 1. N 1s and F 1s spectra are featured in the SI.*

Region	RSF	Composition (%)		
		Before	PS 1	Bulk IL*
C 1s	1.00	73±2	70±1	55.6
N 1s	1.80	9.4±0.3	10.3±0.4	13.2
F 1s	4.43	17±1	19.7±0.4	31.2

* Indicates values adapted from Ref [13] for bulk [C$_4$C$_1$Im][BF$_4$] for comparison to the values from this work.

It should be noted that he relative sensitivity factors in Tables S1 and S2 were obtained from the CasaXPS library, as the equipment was not calibrated for these factors.

Assignments of all composite peaks of all regions

The following table displays the binding energies and assignments of all peaks of all regions displayed both in the main text and in the supporting information.

| Region	Binding Energy (eV) (±0.1 eV)	Assignment
C 1s	285.5	C_1, alkyl chain
	286.8	C_2, imidazolium
	287.0	C_3, imidazolium
	287.9	C_4, imidazolium
N 1s	399.6	Beam damage
	400.9	Beam damage
	402.3	N, imidazolium
O 1s	530.2	TiO_2 substrate
	531.5	Hydroxyl (Ti-OH)
	533.0	Hydroxyl (C-OH)
	533.3	Adsorbed H_2O
	535.9	Gas-phase H_2O
F1s	684.3	F-Ti
	686.4	F, BF_4^-

☐   Indicates peak appears upon exposure to water

Beam damage

Evidence of beam damage appearing in the N 1s spectrum has been reported in numerous works involving imidazolium-based ILs and XPS [4, 14, 15]. However, in this work, beam damage was only evident in the N 1s spectrum and not in the C 1s or F 1s regions as one may expect (F 1s spectra featured earlier in SI). This effect has been seen before in XPS studies of imidazolium ILs [14]. Rastered measurements were taken to minimise sample beam damage, and it can be seen from the N 1s spectra that no extra peaks appear to manifest in the region throughout the experiment. This demonstrates that rastered measurements do somewhat reduce beam damage to IL films. In addition, the peak associated with the N in the imidazolium ring dominates the region throughout the experiment, which shows that that the vast majority of the $[C_4C_1Im]^+$ cations of the IL film remain intact. Water has been known to exacerbate beam damage, and is demonstrated in the beam damage investigation outlined below.

Investigation into beam damage

A short investigation was carried out on the effect of prolonged X-ray exposure on the ultrathin IL film. An IL film was deposited onto the TiO_2 substrate in the same manner as the experiment (also dosed for 30 minutes). Similarly, measurements were taken in three regimes: before exposure to water, during water exposure (at a pressure of 8 mbar and 285 K, which corresponds to a relative humidity of ~70%) and after water exposure. The regime after water exposure was seceded into three measurements, named here as Pump Stages 1 to 3 (similarly abbreviated to PS 1 to PS 3 in all figures). These scans, however, were not rastered. The sample was gently heated in UHV conditions to remove some of the beam-damage species once measurements were taken. As a comparison, the effect of only prolonged X-ray exposure was observed by returning the sample to the in situ cell and subjecting the sample to two more non-rastered measurements, labelled as "beam damage test", or BDT. Each measurement took approximately one hour, and with additional time compensating for sample heating, the experiment overall took eight hours. Fig S5 shows the N 1s region in both investigations.
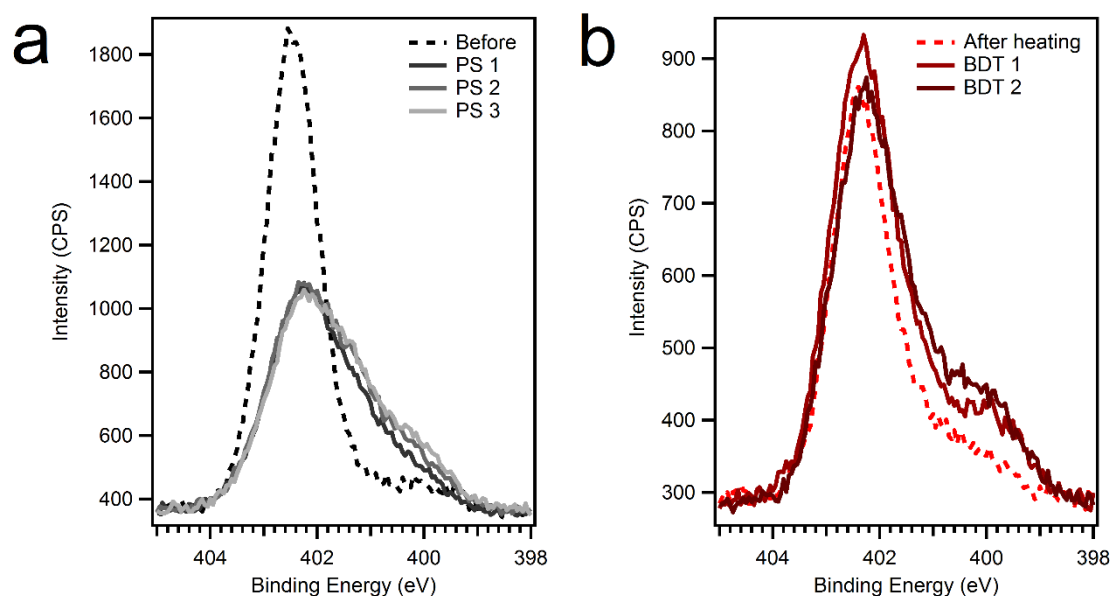
Figure S5. (a) *N 1s region before and after exposure to water, and* **(b)** *N 1s region after heating in UHV and subject to two further scans. The label BDT stands for 'beam damage test'. These measurements were taken on two different areas on the sample, and have not been calibrated.*

The change in shape of the N 1s region is the most dramatic in S5a, where the sample was subject to both water and non-rastered measurements. Throughout PS 1 to PS 3, the sample was no longer surrounded by high-pressure water vapour. The shape of the N 1s region does change throughout PS 1 to PS 3, but it does not change as significantly as in the presence of water vapour. This is supported by the scans shown in S5b, where the sample was only subject to non-raster measurements. While the N 1s region does not return to its original shape (*i.e.* predominantly one signal) after heating, the increase in intensity of the shoulder at lower binding energy is marginal over time compared to that in S5a. Therefore, it can be concluded that water has a significantly exacerbating effect on the beam damage of IL samples.

References

[1] M. Seah, Surface and interface analysis, 44 (2012) 497-503.

[2] C. Han, S. Xia, P. Ma, F. Zeng, Journal of Chemical & Engineering Data, 54 (2009) 2971-2977.

[3] J.F. Watts, J. Wolstenholme, An Introduction to Surface Analysis by XPS and AES, Wiley, 2003.

[4] T. Cremer, M. Stark, A. Deyko, H.-P. Steinrück, F. Maier, Langmuir, 27 (2011) 3662-3671.

[5] M. Mezger, S. Schramm, H. Schröder, H. Reichert, M. Deutsch, E.J. De Souza, J.S. Okasinski, B.M. Ocko, V. Honkimäki, H. Dosch, The Journal of chemical physics, 131 (2009) 094701.

[6] M. Wagstaffe, M.J. Jackman, K.L. Syres, A. Generalov, A.G. Thomas, ChemPhysChem, 17 (2016) 3430-3434.

[7] A. Mele, C.D. Tran, S.H. De Paoli Lacerda, Angewandte Chemie, 115 (2003) 4500-4502.

[8] T. Cremer, M. Killian, J.M. Gottfried, N. Paape, P. Wasserscheid, F. Maier, H.P. Steinruck, ChemPhysChem, 9 (2008) 2185-2190.

[9] I.J. Villar-Garcia, E.F. Smith, A.W. Taylor, F.L. Qiu, K.R.J. Lovelock, R.G. Jones, P. Licence, Physical Chemistry Chemical Physics, 13 (2011) 2797-2808.

[10] L. Cammarata, S.G. Kazarian, P.A. Salter, T. Welton, Physical Chemistry Chemical Physics, 3 (2001) 5192-5200.

[11] S. Rivera-Rubero, S. Baldelli, J. Phys. Chem. B, 110 (2006) 15499-15505.

[12] C. Ridings, V. Lockett, G. Andersson, Physical Chemistry Chemical Physics, 13 (2011) 21301-21307.

[13] E.F. Smith, F.J. Rutten, I.J. Villar-Garcia, D. Briggs, P. Licence, Langmuir, 22 (2006) 9386-9392.

[14] K. Lovelock, C. Kolbeck, T. Cremer, N. Paape, P. Schulz, P. Wasserscheid, F. Maier, H.-P. Steinruck, The Journal of Physical Chemistry B, 113 (2009) 2854-2864.

[15] A. Keppler, M. Himmerlich, T. Ikari, M. Marschewski, E. Pachomow, O. Höfft, W. Maus-Friedrichs, F. Endres, S. Krischok, Physical Chemistry Chemical Physics, 13 (2011) 1174-1181.